
Smooth and Sparse Latent Dynamics in Operator Learning with Jerk Regularization

Anonymous Author(s)

Affiliation

Address

email

Abstract

1 Data-driven latent dynamics models (LDMs) offer a promising approach for fast
2 and accurate spatiotemporal forecasting by computing solutions in a compressed
3 latent space. However, these models often neglect temporal correlations between
4 consecutive snapshots when constructing the latent space, leading to suboptimal
5 compression, jagged latent trajectories, and limited extrapolation ability over time.
6 To address these issues, this paper introduces a continuous operator learning
7 framework that incorporates a novel jerk regularization into the learning of the
8 compressed latent space. This jerk regularization promotes smoothness and sparsity
9 of latent space dynamics, which not only yields enhanced accuracy and convergence
10 speed but also helps identify intrinsic latent space coordinates. The effectiveness of
11 this framework is demonstrated through a two-dimensional unsteady flow problem
12 governed by the Navier-Stokes equations, highlighting its potential to expedite
13 high-fidelity simulations in various scientific and engineering applications.

14 1 Introduction

15 Modeling continuous spatiotemporal dynamics is critical across climate, fluids, biology, and engineering [1, 2, 3, 4]. While governing partial differential equations (PDEs) provide a principled foundation,
16 deriving compact forms is often infeasible [5]. Data-driven surrogate models such as CNN/GNN-
17 based models [6, 7, 8] and operator learning models such as DeepONet and FNO [9, 10, 11, 12, 13, 14]
18 avoid reliance on closed-form PDEs, but both approaches typically rely on autoregressive time
19 stepping, making long-horizon rollouts expensive [15]. In contrast, motivated by the fact that spa-
20 tiotemporal systems often evolve on low-dimensional manifolds [16, 12], latent dynamics models
21 (LDMs) aim to model the dynamics in a compressed latent space learned via an autoencoder, enabling
22 cheaper forecasts than autoregressive operator methods [17, 18, 19, 20, 21, 22, 23, 24, 25, 26].

24 To enhance the robustness and reduce the reliance on large datasets of purely data-driven methods, a
25 promising approach is to embed physical principles such as the PDE itself [27, 28, 29, 30, 20, 31]
26 or general principles such as invariance [32, 33, 34], equivariance [35], symmetry [36, 37], and
27 conservation laws [38]. Among these, *a nearly universal property of physical systems is the temporal*
28 *smoothness of their dynamics*. Thus, phenomena that evolve smoothly over time in the original
29 state space should mirror this smooth trajectory in the reduced latent space. Autoencoders, however,
30 always process data snapshot by snapshot independently, neglecting the temporal correlations between
31 sequential snapshots and overlooking the fact that consecutive snapshots in latent space are likely more
32 similar to each other than to those further away in time or from different trajectories. Prior attempts at
33 integrating smoothness into the learning process either do not explicitly enforce smoothness or prove
34 overly restrictive, penalizing even smooth spiraling trajectories [22, 21, 39]. In this work, we propose
35 a spatiotemporal continuous operator-learning framework that directly minimizes jerk (the time
36 derivative of acceleration) in latent space during autoencoder training, explicitly promoting smooth

37 trajectories and implicitly inducing sparsity without penalties. Through a 2D unsteady Navier-Stokes
 38 example, we show that our jerk regularization yields faster, more accurate convergence for both the
 39 autoencoder and neural-ODE latent dynamics, smoother latent paths, and sparser, more interpretable
 40 coordinates.

41 2 Smooth operator learning

42 We consider a spatiotemporal system described by a PDE of the general form

$$\partial_t u(\mathbf{x}, t) + \mathcal{N}[u(\mathbf{x}, t)] = 0, \quad \mathbf{x} \in \Omega, \quad t \in [0, T], \quad (1)$$

43 where $u(\mathbf{x}, t)$ represents the continuous state of the system in the spatial domain $\Omega \subseteq \mathbb{R}^d$ and temporal
 44 interval $[0, T]$, with \mathcal{N} a potentially unknown nonlinear differential operator. The system is further
 45 subjected to initial and boundary conditions, denoted by $u(\mathbf{x}, 0) = u_0(\mathbf{x})$ and $u(\mathbf{x}_b, t) = g(\mathbf{x}_b, t)$ for
 46 $\mathbf{x}_b \in \partial\Omega$. Our primary goal is to learn the underlying dynamics of (1) from a training dataset, without
 47 requiring knowledge of the operator \mathcal{N} . We assume that the training dataset consists of various
 48 solution trajectories of (1), where the continuous states are discretized in space using a sampling grid
 49 $\{\mathbf{x}_i\}_{i=0}^N$ and in time using a fixed time interval Δt .

50 Our proposed model, depicted in Figure 1, adopts LDM-based continuous operator learning, merging
 51 nonlinear dimensionality reduction with continuous spatiotemporal modeling across space and time.
 52 During the inference stage, a CNN-based encoder transforms the initial high-dimensional system
 53 state $\mathbf{u}(0) = \{u(\mathbf{x}_i, 0)\}_{i=0}^N$ from the ambient space of dimension $N + 1$ into an initial latent vector
 54 $\mathbf{z}(0)$ in a compressed latent space of dimension $d_z \ll N$. Then, the low-dimensional latent vector is
 55 propagated through a neural ODE to compute a future latent vector $\mathbf{z}(t)$ at an arbitrary future time
 56 t . Propagating the latent vector instead of the high-dimensional state significantly accelerates the
 57 inference because the latent dimension d_z is significantly smaller than the ambient space dimension
 58 $N + 1$. Subsequently, a conditional INR-based decoder maps the future latent vector $\mathbf{z}(t)$ back to the
 59 predicted continuous state $\hat{\mathbf{u}}(\mathbf{x}, t)$, enabling predictions at arbitrary spatial and temporal resolutions.

60 The training process is split into two stages. During stage I, illustrated in Figure 1 (b), we train an
 61 autoencoder, consisting of an encoder E_θ with parameters θ and a decoder D_ϕ with parameters ϕ , to
 62 learn an invertible nonlinear map between the ambient space and the compressed latent space. We
 63 employ a standard mean-square-error reconstruction loss L_{recon}^t to ensure that the continuous states
 64 recovered from the decoder are similar to the high-dimensional states given to the encoder. Crucially,
 65 we also ensure that trajectories in latent space are smooth by including a jerk regularization loss that
 66 penalizes the third-order time derivative of the latent vector at each time t , which encourages changes
 67 in acceleration along the latent trajectory to be small without restricting the magnitude and direction
 68 of the velocity and acceleration. Using a finite difference approximation of the acceleration, the jerk
 69 regularization loss L_{jerk}^t at time t is calculated as

$$L_{\text{jerk}}^t = \|\mathbf{z}(t + 3\Delta t) - 3\mathbf{z}(t + 2\Delta t) + 3\mathbf{z}(t + \Delta t) - \mathbf{z}(t)\|_2^2, \quad (2)$$

70 where $\mathbf{z}(t)$, $\mathbf{z}(t + \Delta t)$, $\mathbf{z}(t + 2\Delta t)$, and $\mathbf{z}(t + 3\Delta t)$ are the latent vectors obtained by passing through
 71 the encoder a sequence of high-dimensional states $\mathbf{u}(t)$, $\mathbf{u}(t + \Delta t)$, $\mathbf{u}(t + 2\Delta t)$, and $\mathbf{u}(t + 3\Delta t)$
 72 belonging to the same solution trajectory, and $\|\cdot\|_2$ denotes the L_2 norm of the vector. The total
 73 loss at time t for the training of the autoencoder is $L = L_{\text{recon}}^t + \lambda L_{\text{jerk}}^t$, where the scalar weight λ
 74 controls the strength of the jerk regularization.

75 Once the autoencoder is trained, we convert ambient space snapshots across all trajectories from the
 76 training dataset into their latent space representations. The resulting dataset of latent trajectories then
 77 serves as the basis for training the neural ODE during the training stage II, which is shown in Figure 1
 78 (c). The neural ODE $\partial_t \mathbf{z}(t) = h_\psi[\mathbf{z}(t)]$ with parameters ψ is trained to learn the temporal evolution
 79 of latent vectors using a mean square error loss on whole trajectory rollouts. Finally, our final trained
 80 model enables predictions at any point in space and time, similar to other recent methods using both
 81 conditional INRs and neural ODEs [18, 40, 22, 19].

82 3 Results

83 We demonstrate the effectiveness of the proposed framework on a 2D problem governed by the incom-
 84 pressible Navier-Stokes equations in vorticity form with an added volume force term, corresponding

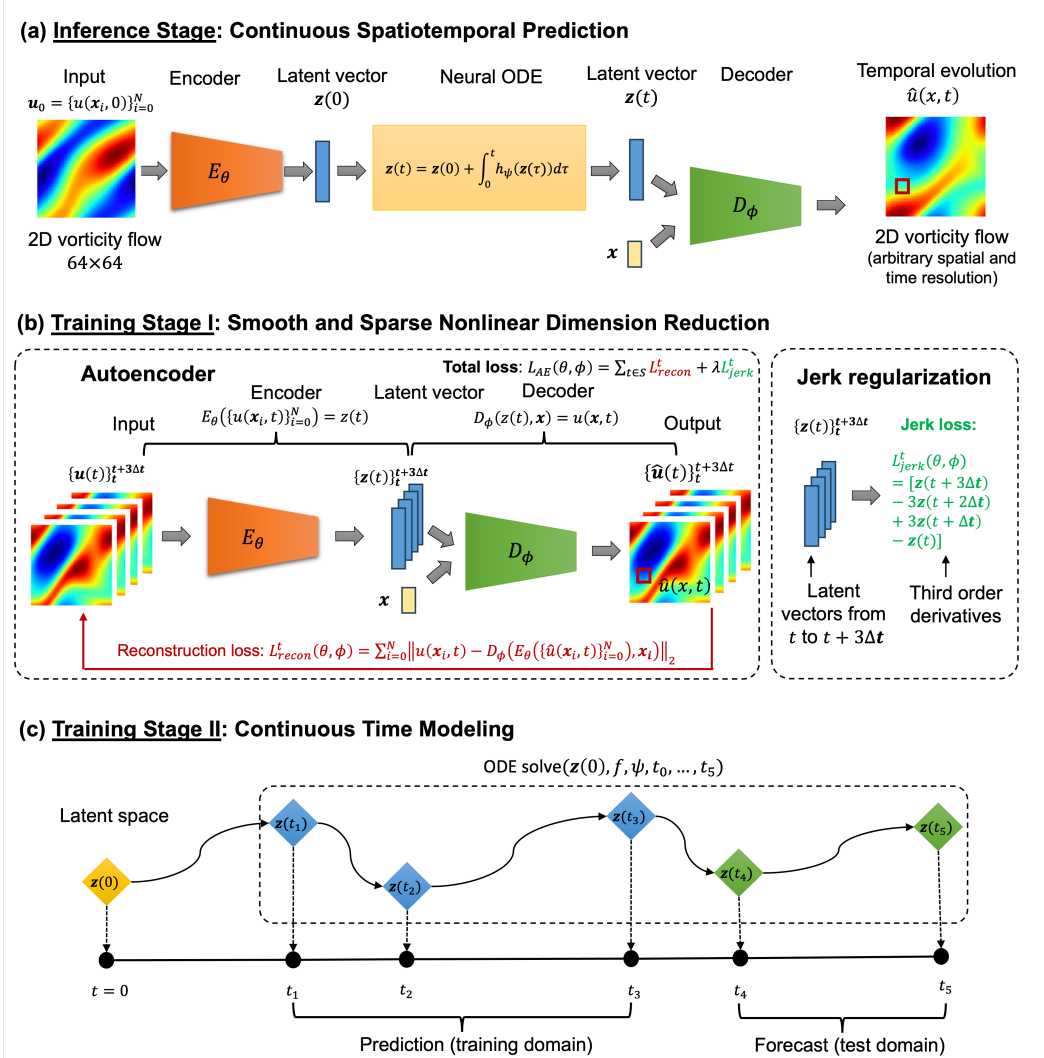


Figure 1: **Schematic of our smooth operator learning model.** (a) **Inference Stage:** The encoder transforms the initial system state $u(0)$ into a compressed latent vector $z(0)$, which is evolved through a neural ODE into a prediction $z(t)$ at any subsequent time t . A conditional INR decoder then reconstructs the predicted continuous system state $u(x, t)$ from $z(t)$. (c) **Training Stage I:** The autoencoder learns a mapping between original and compressed latent spaces. A jerk regularization loss enforces smoothness of trajectories in latent space. (c) **Training Stage II:** The neural ODE is trained to learn a continuous-time model of the dynamics within the latent space.

to the $Re = 1000$ dataset investigated in the original FNO paper [9]. The original resolution of the simulation data is 256×256 , which we downsampled to 64×64 . Each trajectory contains 51 time steps with $\Delta t = 1$. We removed the initial 10 time steps due to inherent noise and diminished relevance to the underlying dynamics. The data from time $t = 11$ to $t = 40$ is designated for training, while data from $t = 41$ to $t = 50$ is set aside for time extrapolation testing. Of the 1000 total trajectories, 900 trajectories were used for training, and the remaining 100 trajectories for testing. We set the latent space dimension to $d_z = 32$.

Figure 2 displays the effect of jerk regularization on the trajectories in latent space. The left panel depicts a latent space trajectory in the test set obtained from an autoencoder trained after stage I without jerk regularization ($\lambda = 0$). The trajectory is visualized in terms of the time series of the components of the latent vector, which exhibit nonphysical jerkiness. The right panel shows that including jerk regularization ($\lambda = 0.1$) when training the autoencoder leads to a markedly smoother

97 latent space trajectory, with a 35-fold drop in the average jerk metric, given by the average jerk loss
 98 over all time steps. Interestingly, jerk regularization also encourages sparsity of the latent vector, with
 99 most latent coordinates remaining constant over time. This suggests that jerk regularization may help
 100 selecting an optimal latent space dimension.

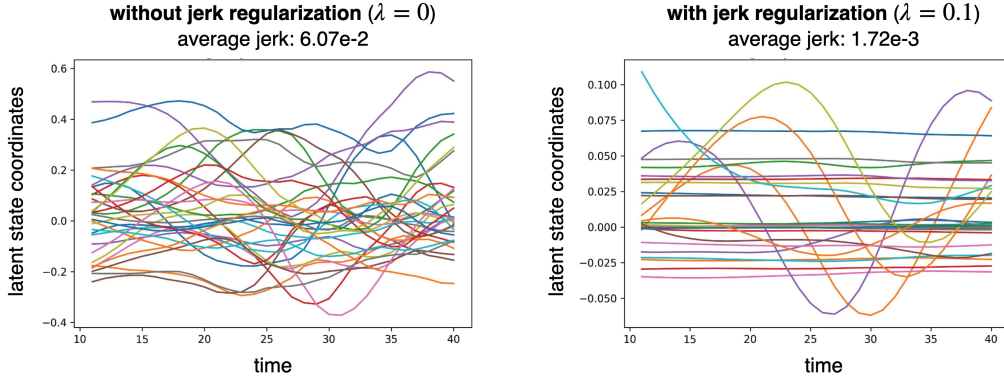


Figure 2: **Comparison of a latent space trajectory obtained with and without jerk regularization.**
 Jerk regularization yields smoother and sparser latent trajectories.

101 Figure 3 shows that the jerk regularization not
 102 only helps the autoencoder learn smoother la-
 103 tent space trajectories, but it yields increased
 104 accuracy of the reconstructed states.

105 Finally, Figure 4 demonstrates that jerk regu-
 106 larization markedly improves the predictive ac-
 107 curacy of the final model obtained after train-
 108 ing stages I and II, including beyond the train-
 109 ing time domain. This improvement is due to
 110 the lower autoencoder reconstruction error as
 111 well as more accurate neural ODE training from
 112 smooth trajectories.

113 Overall, our smoothness-promoting jerk regu-
 114 larization shows potential to improve the per-
 115 formance of surrogate models for spatiotemporal dynamics. Future work will include evaluating the
 116 applicability of this technique across various physical systems.

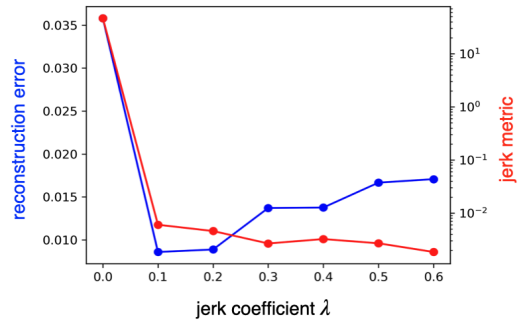


Figure 3: Reconstruction error and jerk metric for test trajectories versus jerk loss weight λ .

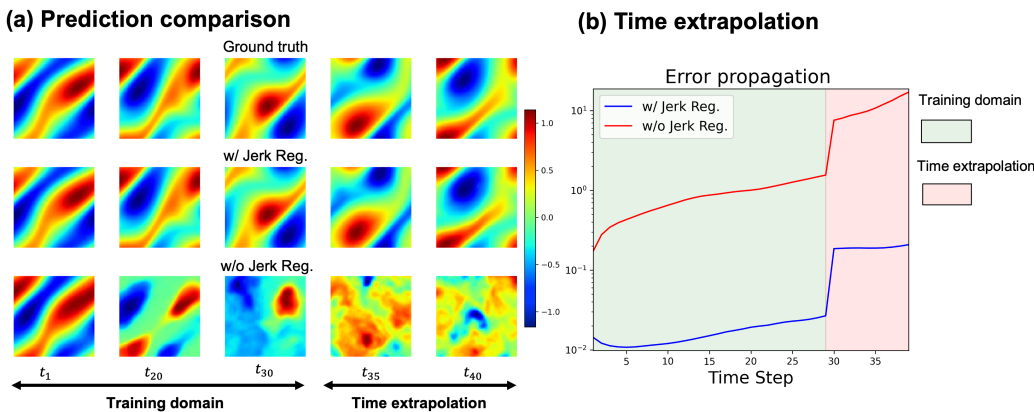


Figure 4: **Comparison of ground truth vorticity fields and model predictions.** (a) Time interpola-
 tion and extrapolation comparisons in the test set. (b) Relative mean square error (RMSE) inside
 (green area) and outside (pink area) the training time domain.

117 **References**

- 118 [1] Kaifeng Bi, Lingxi Xie, Hengheng Zhang, Xin Chen, Xiaotao Gu, and Qi Tian. Accurate
119 medium-range global weather forecasting with 3d neural networks. *Nature*, 619(7970):533–538,
120 2023.
- 121 [2] Steven L Brunton, Bernd R Noack, and Petros Koumoutsakos. Machine learning for fluid
122 mechanics. *Annual review of fluid mechanics*, 52:477–508, 2020.
- 123 [3] Mark Alber, Adrian Buganza Tepole, William R Cannon, Suvarnu De, Salvador Dura-Bernal,
124 Krishna Garikipati, George Karniadakis, William W Lytton, Paris Perdikaris, Linda Petzold,
125 et al. Integrating machine learning and multiscale modeling—perspectives, challenges, and
126 opportunities in the biological, biomedical, and behavioral sciences. *NPJ digital medicine*,
127 2(1):115, 2019.
- 128 [4] Mojtaba Mozaffar, Shuheng Liao, Xiaoyu Xie, Sourav Saha, Chanwook Park, Jian Cao,
129 Wing Kam Liu, and Zhengtao Gan. Mechanistic artificial intelligence (mechanistic-ai) for mod-
130eling, design, and control of advanced manufacturing processes: Current state and perspectives.
131 *Journal of Materials Processing Technology*, 302:117485, 2022.
- 132 [5] Steven L Brunton, Joshua L Proctor, and J Nathan Kutz. Discovering governing equations
133 from data by sparse identification of nonlinear dynamical systems. *Proceedings of the national
134 academy of sciences*, 113(15):3932–3937, 2016.
- 135 [6] Pu Ren, Chengping Rao, Yang Liu, Jian-Xun Wang, and Hao Sun. Phycrnet: Physics-informed
136 convolutional-recurrent network for solving spatiotemporal pdes. *Computer Methods in Applied
137 Mechanics and Engineering*, 389:114399, 2022.
- 138 [7] Chengping Rao, Pu Ren, Qi Wang, Oral Buyukozturk, Hao Sun, and Yang Liu. Encoding
139 physics to learn reaction-diffusion processes. *Nature Machine Intelligence*, pages 1–15, 2023.
- 140 [8] Tobias Pfaff, Meire Fortunato, Alvaro Sanchez-Gonzalez, and Peter W Battaglia. Learning
141 mesh-based simulation with graph networks. *arXiv preprint arXiv:2010.03409*, 2020.
- 142 [9] Zongyi Li, Nikola Kovachki, Kamyar Azizzadenesheli, Burigede Liu, Kaushik Bhattacharya,
143 Andrew Stuart, and Anima Anandkumar. Fourier neural operator for parametric partial differen-
144 tial equations. *arXiv preprint arXiv:2010.08895*, 2020.
- 145 [10] Lu Lu, Pengzhan Jin, Guofei Pang, Zhongqiang Zhang, and George Em Karniadakis. Learning
146 nonlinear operators via deeponet based on the universal approximation theorem of operators.
147 *Nature machine intelligence*, 3(3):218–229, 2021.
- 148 [11] Jaideep Pathak, Shashank Subramanian, Peter Harrington, Sanjeev Raja, Ashesh Chattopadhyay,
149 Morteza Mardani, Thorsten Kurth, David Hall, Zongyi Li, Kamyar Azizzadenesheli, et al.
150 Fourcastnet: A global data-driven high-resolution weather model using adaptive fourier neural
151 operators. *arXiv preprint arXiv:2202.11214*, 2022.
- 152 [12] Jacob Seidman, Georgios Kissas, Paris Perdikaris, and George J Pappas. Nomad: Nonlinear
153 manifold decoders for operator learning. *Advances in Neural Information Processing Systems*,
154 35:5601–5613, 2022.
- 155 [13] Tapas Tripura and Souvik Chakraborty. Wavelet neural operator for solving parametric partial
156 differential equations in computational mechanics problems. *Computer Methods in Applied
157 Mechanics and Engineering*, 404:115783, 2023.
- 158 [14] Georgios Kissas, Jacob H Seidman, Leonardo Ferreira Guilhoto, Victor M Preciado, George J
159 Pappas, and Paris Perdikaris. Learning operators with coupled attention. *The Journal of Machine
160 Learning Research*, 23(1):9636–9698, 2022.
- 161 [15] Johannes Brandstetter, Daniel Worrall, and Max Welling. Message passing neural pde solvers.
162 *arXiv preprint arXiv:2202.03376*, 2022.
- 163 [16] Albert Cohen and Ronald DeVore. Approximation of high-dimensional parametric pdes. *Acta
164 Numerica*, 24:1–159, 2015.

- 165 [17] Kookjin Lee and Kevin T Carlberg. Model reduction of dynamical systems on nonlinear mani-
 166 folds using deep convolutional autoencoders. *Journal of Computational Physics*, 404:108973,
 167 2020.
- 168 [18] Peter Yichen Chen, Jinxu Xiang, Dong Heon Cho, Yue Chang, GA Pershing, Henrique Teles
 169 Maia, Maurizio M Chiaramonte, Kevin Thomas Carlberg, and Eitan Grinspun. Crom: Contin-
 170 uous reduced-order modeling of pdes using implicit neural representations. In *The Eleventh*
 171 *International Conference on Learning Representations*, 2022.
- 172 [19] Yuan Yin, Matthieu Kirchmeyer, Jean-Yves Franceschi, Alain Rakotomamonjy, and Patrick
 173 Gallinari. Continuous pde dynamics forecasting with implicit neural representations. In *The*
 174 *Eleventh International Conference on Learning Representations*, 2023.
- 175 [20] Aleksei Sholokhov, Yuying Liu, Hassan Mansour, and Saleh Nabi. Physics-informed neural
 176 ode (pinode): embedding physics into models using collocation points. *Scientific Reports*,
 177 13(1):10166, 2023.
- 178 [21] Xiaolong He, Youngsoo Choi, William D Fries, Jonathan L Belof, and Jiun-Shyan Chen.
 179 Glasdi: Parametric physics-informed greedy latent space dynamics identification. *Journal of*
 180 *Computational Physics*, page 112267, 2023.
- 181 [22] Zhong Yi Wan, Leonardo Zepeda-Núñez, Anudhyana Boral, and Fei Sha. Evolve smoothly, fit
 182 consistently: Learning smooth latent dynamics for advection-dominated systems. *arXiv preprint*
 183 *arXiv:2301.10391*, 2023.
- 184 [23] Louis Serrano, Lise Le Boudec, Armand Kassaï Koupaï, Thomas X Wang, Yuan Yin, Jean-Noël
 185 Vittaut, and Patrick Gallinari. Operator learning with neural fields: Tackling pdes on general
 186 geometries. *arXiv preprint arXiv:2306.07266*, 2023.
- 187 [24] Ryan V Raut, Zachary P Rosenthal, Xiaodan Wang, Hanyang Miao, Zhanqi Zhang, Jin-Moo
 188 Lee, Marcus E Raichle, Adam Q Bauer, Steven L Brunton, Bingni W Brunton, et al. Arousal as
 189 a universal embedding for spatiotemporal brain dynamics. *bioRxiv*, pages 2023–11, 2023.
- 190 [25] Samuel E Otto, Gregory R Macchio, and Clarence W Rowley. Learning nonlinear projections
 191 for reduced-order modeling of dynamical systems using constrained autoencoders. *Chaos: An*
 192 *Interdisciplinary Journal of Nonlinear Science*, 33(11), 2023.
- 193 [26] Peiyi Chen, Tianchen Hu, and Johann Guilleminot. A nonlinear-manifold reduced-order model
 194 and operator learning for partial differential equations with sharp solution gradients. *Computer*
 195 *Methods in Applied Mechanics and Engineering*, 419:116684, 2024.
- 196 [27] Xiaoyu Zhao, Zhiqiang Gong, Yunyang Zhang, Wen Yao, and Xiaoqian Chen. Physics-informed
 197 convolutional neural networks for temperature field prediction of heat source layout without
 198 labeled data. *Engineering Applications of Artificial Intelligence*, 117:105516, 2023.
- 199 [28] Zongyi Li, Hongkai Zheng, Nikola Kovachki, David Jin, Haoxuan Chen, Burigede Liu, Kamkar
 200 Azizzadenesheli, and Anima Anandkumar. Physics-informed neural operator for learning partial
 201 differential equations. *arXiv preprint arXiv:2111.03794*, 2021.
- 202 [29] Sifan Wang, Hanwen Wang, and Paris Perdikaris. Learning the solution operator of para-
 203 metric partial differential equations with physics-informed deeponets. *Science advances*,
 204 7(40):eabi8605, 2021.
- 205 [30] Somdatta Goswami, Aniruddha Bora, Yue Yu, and George Em Karniadakis. Physics-informed
 206 deep neural operator networks. In *Machine Learning in Modeling and Simulation: Methods*
 207 *and Applications*, pages 219–254. Springer, 2023.
- 208 [31] N Navaneeth, Tapas Tripura, and Souvik Chakraborty. Physics informed wno. *Computer*
 209 *Methods in Applied Mechanics and Engineering*, 418:116546, 2024.
- 210 [32] Julia Ling, Reese Jones, and Jeremy Templeton. Machine learning strategies for systems with
 211 invariance properties. *Journal of Computational Physics*, 318:22–35, 2016.

- 212 [33] Julia Ling, Andrew Kurzawski, and Jeremy Templeton. Reynolds averaged turbulence modelling
213 using deep neural networks with embedded invariance. *Journal of Fluid Mechanics*, 807:155–
214 166, 2016.
- 215 [34] Xiaoyu Xie, Arash Samaei, Jiachen Guo, Wing Kam Liu, and Zhengtao Gan. Data-driven
216 discovery of dimensionless numbers and governing laws from scarce measurements. *Nature
217 communications*, 13(1):7562, 2022.
- 218 [35] Soledad Villar, David W Hogg, Kate Storey-Fisher, Weichi Yao, and Ben Blum-Smith. Scalars
219 are universal: Equivariant machine learning, structured like classical physics. *Advances in
220 Neural Information Processing Systems*, 34:28848–28863, 2021.
- 221 [36] Alex Gabel, Victoria Klein, Riccardo Valperga, Jeroen SW Lamb, Kevin Webster, Rick Quax,
222 and Efstratios Gavves. Learning lie group symmetry transformations with neural networks. In
223 *Topological, Algebraic and Geometric Learning Workshops 2023*, pages 50–59. PMLR, 2023.
- 224 [37] Hee-Sun Choi, Yonggyun Yu, and Hogeon Seo. Symmetry-informed surrogates with data-free
225 constraint for real-time acoustic wave propagation. *Applied Acoustics*, 214:109686, 2023.
- 226 [38] Derek Hansen, Danielle C Maddix, Shima Alizadeh, Gaurav Gupta, and Michael W Mahoney.
227 Learning physical models that can respect conservation laws. *arXiv preprint arXiv:2302.11002*,
228 2023.
- 229 [39] Saaketh Desai, Ankit Shrivastava, Marta D’Elia, Habib N Najm, and Rémi Dingreville. Trade-
230 offs in the latent representation of microstructure evolution. *Acta Materialia*, 263:119514,
231 2024.
- 232 [40] Shaowu Pan, Steven L Brunton, and J Nathan Kutz. Neural implicit flow: a mesh-agnostic
233 dimensionality reduction paradigm of spatio-temporal data. *Journal of Machine Learning
234 Research*, 24(41):1–60, 2023.